Magazine of Concrete Research, 2010, **62**, No. 4, April, 267–282
doi: 10.1680/macr.2010.62.4.267

Shear design of short-span beams

J. Sagaseta* and R. L. Vollum†

École Polytechnique Fédérale de Lausanne; Imperial College London

Eurocode 2 presents two alternative methods for accounting for arching action in beams. The simplest option is to reduce the component of shear force owing to loads applied within 2d of the support by the multiple $a_v/2d$ (where a_v is the clear shear span and d is the effective depth). Eurocode 2 also allows short-span beams to be designed with the strut-and-tie method (STM), raising the question of which method to use. This paper presents a simple strut-and-tie model for short-span beams. The stress fields used in the STM are shown to be broadly consistent with those calculated with non-linear finite-element analysis. The STM is shown to give good predictions of shear strength, particularly when the concrete strength is calculated in accordance with the recommendations of Collins and Mitchell. The accuracy of the simplified design method in Eurocode 2 is shown to be highly dependent on the stirrup index. The paper also presents data from eight beams tested by the authors which show that aggregate fracture has little if any influence on the shear strength of short-span beams.

Notation

A_{sl}	area of longitudinal reinforcement
A_{sw}	area of steel provided by each stirrup
a	shear span between centre line of bearing plates
a_v	clear shear span between inner edges of plates
b	beam width
C'_i	vertical distance from top of the beam to the centreline of indirect strut III at stirrup i
c	distance from bottom of the beam to centroid of flexural reinforcement
d	effective depth
$\boldsymbol{f}'_c$	concrete cylinder strength
$\boldsymbol{f}_{csb}$	concrete strength in direct strut at bottom node
$\boldsymbol{f}_{cnt}$	concrete strength at top node
$\boldsymbol{f}_{yd}$	design yield strength of reinforcement
h	overall height of the beam ($h = d + c$)
l_b	length of bottom bearing plate
l_t	length of top bearing plate
n	number of effective stirrups
n_{lp}	number of loading points (1 or 2)
P	total load
S_i	distance from stirrup to rear face of the top node
SI	stirrup index defined for short-span beams SI $= nA_{sw}f_y/(bhf'_c)$
T_d	longitudinal force transmitted to bottom node by direct strut I
T'_i	longitudinal force transmitted to bottom node by indirect strut III
T_{si}	force resisted by each stirrup
V	shear force
V_c	concrete component of shear resistance
V_d	shear contribution of direct strut
V_s	stirrup contribution to shear
$V_{Rd,c}$	shear strength of member without shear reinforcement
w_{strut}	strut width at bottom node
z	lever arm (0·9d for shear in Eurocode 2)
β	fraction of total tensile force transferred by direct strut to bottom node in strut-and-tie model
γ_c, γ_s	partial factors for concrete and steel respectively
ε_L	principal tensile strength in concrete
ε_l	strain in tie
θ	inclination of direct strut
λ	fraction of shear carried by direct strut in strut-and-tie model
ν	strength reduction factor for cracked concrete in shear
ρ_l	longitudinal reinforcement ratio $\rho_l = A_{sl}/(bd)$
σ	stress in concrete at node boundary
ϕ'_i	angle to the horizontal made by a line drawn from the top of stirrup i to the bottom of the node

* École Polytechnique Fédérale de Lausanne (EPFL), Lausanne, Switzerland
† Department of Civil and Environmental Engineering Imperial College, London, UK

(MACR 900100) Paper received 17 June 2009; accepted 24 July 2009

www.concrete-research.com 1751-763X (Online) 0024-9831 (Print)

Introduction

Considerable experimental work has been carried out over the past 50 years into the shear behaviour of reinforced concrete (RC) beams, with particular emphasis on slender beams with shear span to effective depth ratios $a_v/d > 2$ (where a_v is the clear shear span and d is the effective depth) and on deep beams with $a_v/d < 1$. Short-span beams with a_v/d ratios ranging from 1 to 2, have been studied to a lesser extent. It is well known that the shear strength of RC beams increases significantly owing to arching action when loads are applied within approximately twice the beams' effective depth of the support. The behaviour of short-span beams differs significantly from slender and deep beams. When a_v/d is between 1 and 2, the diagonal crack forms independently of flexural cracks and the beam remains stable after the formation of the diagonal crack, which typically runs between the inner edges of the bearing plates (see Figure 1). The shear strength and ductility of short-span beams can be enhanced by adding transverse reinforcement. Kong *et al.* (1970) have shown that vertical stirrups are more efficient than horizontal links for $a_v/d > 1$. Vertical stirrups increase shear strength if they cross the diagonal shear crack and are considered effective for design purposes if placed within the central three quarters of the clear shear span a_v. It is convenient to define the effective amount of transverse reinforcement in short-span beams in terms of a stirrup index $\mathrm{SI} = nA_{sw}\,\boldsymbol{f}_y/(bhf'_c)$, where n is the number of stirrups within the central three quarters of the clear shear span a_v, A_{sw} is the area of steel provided by each stirrup, $\boldsymbol{f}_y$ is the yield strength of steel, b is the beam width, h is the overall height and $\boldsymbol{f}'_c$ is the concrete cylinder strength.

Existing design methods

Short-span beams without shear reinforcement

Eurocode 2 (BSI, 2004) uses Equation 1 to determine the shear strength of slender beams without shear reinforcement

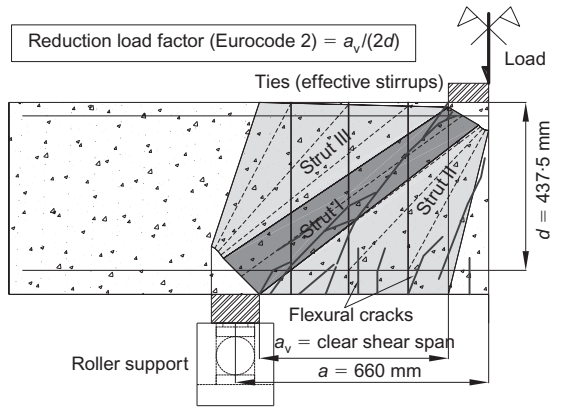

Figure 1. Typical crack pattern and load paths in a short span beam $1 < a_v/d < 2$ with stirrups (beam AL3, tested by the authors at Imperial College London)

$$V_{Rd,c} = \frac{0{\cdot}18}{\gamma_c}(100.\rho_l\,\boldsymbol{f}_{ck})^{1/3}\left(1+\sqrt{200/d}\right)bd \qquad (1)$$

where γ_c is the partial factor for concrete which equals 1·5, $\rho_l = A_{sl}/(bd)$; $\boldsymbol{f}_{ck}$ is the concrete cylinder strength; d is effective depth; and b is member width.

Equation 1 accounts semi-rationally for size effects, dowel action, reinforcement ratio and concrete strength. Eurocode 2 reduces the design shear force by the multiple a_v/2d to account for the increase in shear strength due to arching action in short-span beams. BS 8110 (BSI, 1997) adopts the alternative approach of multiplying the basic shear resistance V_c, which is calculated similarly to $V_{Rd,c}$ in Eurocode 2, by an 'enhancement' factor equal to $2d/a_v$.

Design of short-span beams with vertical shear reinforcement

Model Code 1990 (MC90 (CEB–FIP, 1993)). MC90 uses Equation 2 below, which was initially proposed by Schlaich *et al.* (1987), for the design of vertical shear reinforcement in short-span beams

$$F_w = \frac{2a/z - 1}{3 - N_{Sd}/F}F \qquad (2)$$

where F_w is the design shear force for the stirrups, F is the design shear force, a is the distance between the centre line of the applied load F and the support, z is the lever arm (0·9d where d is the effective depth) and N_{Sd} is axial force (tension positive). It is noteworthy that F_w only depends on a/z and not the stirrup index $\mathrm{SI} = nA_{sw}\,\boldsymbol{f}_y/(bh\boldsymbol{f}'_c)$ which is inconsistent with the experimental results presented in this paper.

Eurocode 2. When loads are applied within 2d of the support, Eurocode 2 reduces the component of the shear force owing to loads applied within 2d of the support by the multiple a_v/2d. For vertical stirrups, the design shear resistance calculated this way equals

$$V_{Ed} = \mathrm{Maximum}(\Sigma A_{sw}\,\boldsymbol{f}_{yd},\ V_{Rdc}) \qquad (3)$$

where $\Sigma A_{sw}\boldsymbol{f}_{yd}$ is the resistance of the shear reinforcement within the central three quarters of the shear span and V_{Rdc} is given by Equation 1.

Standard truss (BS 8110). BS 8110 takes the design shear strength as $V = V_c + V_s$ where V_c is the design shear strength without stirrups and V_s is the contribution of the shear reinforcement which is calculated with a 45° truss. BS 8110 increases the concrete contribution V_c by the multiple $2d/a_v$ when $a_v < 2$d.

Modified truss ($V_d + V_s$). The 45° truss used in BS 8110 would seem to underestimate the contribution of the shear reinforcement in short-span beams since the inclined shear crack typically extends between the loaded areas. In this case, the contribution

of the shear reinforcement $V_s = nA_{sw}f_y$ where n is the effective number of stirrups within the shear span. Consideration of vertical equilibrium suggests that the shear strength equals $V_d + V_s$ where V_d is the contribution of the direct strut (i.e. arching action) and V_s is the contribution of the stirrups. The modified truss gives a notional upper bound to the shear capacity if V_d is taken as $V_{Rdc}(2d/a_v)$ where V_{Rdc} is calculated with Equation 1.

Proposed strut-and-tie model for short-span beams

Eurocode 2 allows short-span beams to be designed using the strut-and-tie method (STM). The STM presented in this section is applicable to symmetrically loaded beams with either one or two point loads ($n_{lp} = 1$ or 2). The geometry of the authors' strut-and-tie model is defined in Figure 2. The bearing stress under the loading and supporting plates was limited to νf_{cd} and $0{\cdot}85\nu \boldsymbol{f}_{cd}$ respectively as recommended in Eurocode 2 for compression–compression (CC) and compression–tension (CT) nodes. The stress distribution is assumed to be non-hydrostatic in the nodes and to be uniformly distributed across the width of the node faces as shown in Figure 2. The load is assumed to be transferred from the loading plate to the supports through a direct strut (strut I) acting in parallel with the truss system (strut II–stirrups–strut III) shown in Figure 1. The stirrups are assumed to yield at failure as observed in the tests of Clark (1951), Regan (1971) and others for stirrup indices up to around 0·1.

The strength of struts I and II is reduced by cracking and transverse tensile strains induced by the stirrups. Strut III, is fan shaped like strut II, but the concrete in this region is essentially uncracked. The failure load P can be defined in terms of the tensile strength of the effective stirrups as follows

$$P = \frac{2}{(1-\lambda)} . \sum_{1}^{n} T_{Si} \tag{4}$$

where $\sum_1^n T_{Si}$ is the sum of the forces T_{Si} resisted by each stirrup ($T_{Si} = A_{sw}\boldsymbol{f}_y$) and n is the number of effective stirrups which is defined as the number within the central three-quarters of the shear span a_v. The proportion of the shear force taken by the direct strut (strut I) is defined by λ. The force in the tensile reinforcement at the bottom node (T) can be subdivided into two components $T = T_i' + T_d$, where T_i' and T_d, respectively, equal the longitudinal component of force in strut III and the direct strut

$$T_i' = T_{Si} . \sum_{1}^{n} \cot \phi_i' \tag{5}$$

$$T_d = \beta T \tag{6}$$

$$T_d = \frac{\lambda}{1-\lambda} . \cot\theta . \sum_{1}^{n} T_{Si} = \frac{\beta T_i'}{1-\beta} \tag{7}$$

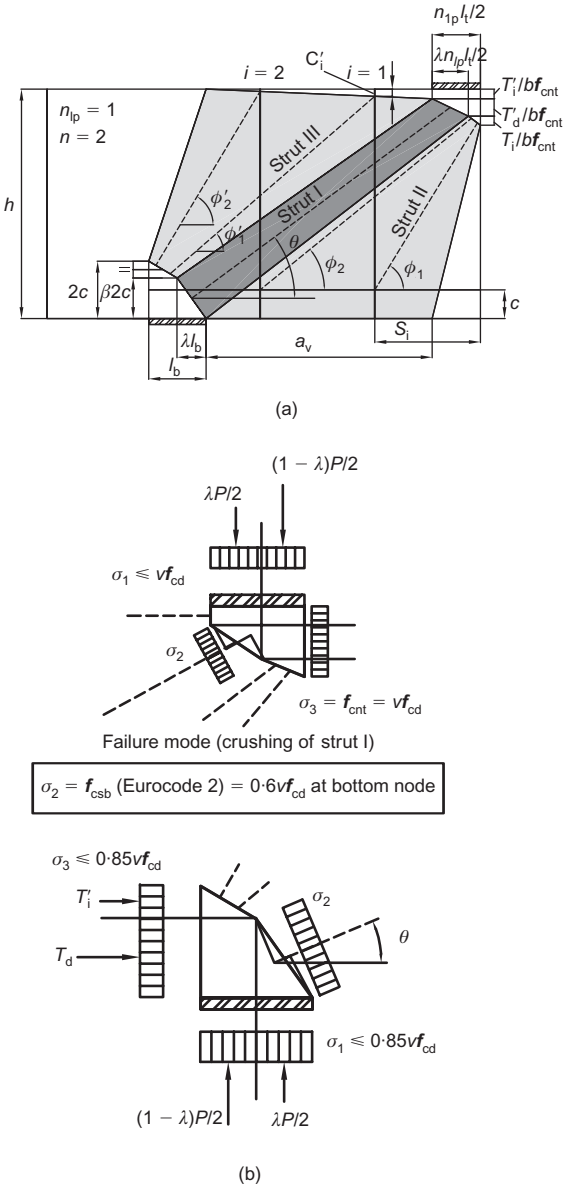

Figure 2. (a) Proposed strut-and-tie model for short span beams with vertical shear reinforcement (example for one point loading and two stirrups; $n_{lp} = 1$ and $n = 2$); (b) stresses at nodal regions

where ϕ_i' is the angle to the horizontal made by a line drawn from the top of stirrup i to the bottom node as shown in Figure 2, and θ is angle of inclination of the centreline of the direct strut to the horizontal. The angles θ and ϕ_i' are defined as follows

$$\cot\theta = \frac{a_v + (l_b\lambda/2) + (l_t\lambda/4)n_{lp}}{h - c\beta - \{[(T_i' + T_d/2)/bf_{cnt}]\}} \tag{8}$$

$$\cot\phi_i' = \frac{a_v + l_b - \{[2(n-i)+1]/2n\}}{h - 2c + ([2(n-i)+1/2n])} \frac{(1-\lambda).l_b - S_i + (l_t/2)n_{lp}}{(1-\beta).2c - C_i'} \tag{9}$$

where a_v is the clear shear span, n_{lp} is the number of loading points at the top of the beam (1 or 2), $l_b - l_t$ is

the length of the bottom–top bearing plates respective, h is height, c is the distance to the centroid of the longitudinal reinforcement, $\boldsymbol{f}_{\mathrm{cnt}}$ is the concrete strength at the top node which is assumed to equal $\nu\boldsymbol{f}_{\mathrm{cd}}$, n is the number of stirrups, b is the beam width, i is the stirrup number, S_i is the distance from stirrup i to the rear face of the top node and C_i' is the vertical distance from the top of the beam to the intersection of the centreline of indirect strut III with stirrup i.

The upper boundary of strut III is assumed to be linear to simplify the calculation of C_i' which is given by

$$C_i' = \frac{T_{\mathrm{i}}'}{b\boldsymbol{f}_{\mathrm{cnt}}} \cdot \frac{a_{\mathrm{v}} - S_i + l_{\mathrm{t}} n_{\mathrm{lp}}/2}{a_{\mathrm{v}}} \tag{10}$$

The geometry of the bottom node is completely defined in terms of the length of the bearing plate (l_{b}) and $2c$ (where c is defined in Figure 2) once λ and β (see Equation 6) are known. The ultimate load is taken as the lowest value corresponding to either flexural failure, crushing of the direct strut or bearing failure. Crushing of the direct strut was the critical failure mode in the majority of beams studied in this paper. The strength of the direct strut is given by the least product of its cross-sectional area and the effective concrete strength. The strength of concrete in the strut is reduced by the effects of cracking and transverse tensile strain. Eurocode 2 defines the design concrete strength in the strut as $0{\cdot}6\nu\boldsymbol{f}_{\mathrm{cd}}$ where $\nu = (1 - \boldsymbol{f}_{\mathrm{ck}}/250)$ and $\boldsymbol{f}_{\mathrm{cd}} = \boldsymbol{f}_{\mathrm{ck}}/\gamma_{\mathrm{c}}$. Alternatively, Collins and Mitchell (1991) propose that the concrete strength in the strut ($\boldsymbol{f}_{\mathrm{csb}}$) should be taken as

$$\boldsymbol{f}_{\mathrm{csb}} = \phi\,\boldsymbol{f}_{\mathrm{ck}}/(0{\cdot}8 + 170\varepsilon_1) \tag{11}$$

where ϕ is a capacity reduction factor and

$$\varepsilon_1 = \varepsilon_L + (\varepsilon_L + 0{\cdot}002)\cot^2\theta \tag{12}$$

where ε_L is the strain in the tie.

Both of these approaches are compared in this paper. The STM was found to give good results if the strength of the direct strut was calculated in terms of its width at the bottom node ($w_{s\mathrm{trut}}$)

$$w_{\mathrm{strut}} = \lambda l_{\mathrm{b}} \sin\theta + 2c\beta\cos\theta \tag{13}$$

Limiting the stress in the strut to $\boldsymbol{f}_{\mathrm{csb}}$ and imposing vertical equilibrium at the bottom node leads to

$$\frac{\lambda}{1-\lambda} \cdot \sum_{1}^{n} T_{\mathrm{Si}} = \left(\lambda l_{\mathrm{b}} \sin^2\theta + c\beta\sin 2\theta\right) b\boldsymbol{f}_{\mathrm{csb}} \tag{14}$$

Equations 4–10 and Equation 14 can be solved for P or A_{sw} as required using an iterative solution procedure. Solving Equations 4–10 and Equation 14 in their general form allows the spacing of the vertical reinforcement to be modelled. The solution procedure is simplified if the stirrups are assumed to be uniformly distributed within the shear span with the resultant stirrup force located at the centre of the clear shear span. In this case, Equations 4–10 and Equation 14 can be solved with the algorithm shown in Figure 3 if the stresses under the loading and supporting plates are less than $\nu\boldsymbol{f}_{\mathrm{cd}}$ and $0{\cdot}85\nu\boldsymbol{f}_{\mathrm{cd}}$ respectively. The algorithm in Figure 3 typically gives very similar solutions to the rigorous procedure described above in which the actual stirrup positions are modelled.

It should be noted that the parameter λ_i which defines the proportion of load resisted by the direct strut, decreases with the increasing stirrup index. The increase in strength owing to stirrups is mainly attributable to the resulting reorientation in the geometry of the bottom node. For large values of SI, λ can become zero in which case the direct strut vanishes making the model no longer applicable. It is questionable whether all the stirrups yield at failure as assumed in the model when $\lambda = 0$. The minimum stirrup index at which $\lambda = 0$, $\mathrm{SI}_{\mathrm{max}} = P_{\mathrm{max}}/(2bh\boldsymbol{f}_{\mathrm{c}})$ can be found by solving Equations 15 and 16. These equations were derived by differentiating Equation 13 with respect to λ and substituting $\lambda = \beta = 0$ into Equations 4 to 10 to obtain the load at which the direct strut disappears.

$$P_{\mathrm{max}} = 2\left(\frac{l_{\mathrm{b}} + 2c\left(\cot^2\theta/\cot\phi'\right)}{1 + \cot^2\theta}\right) b\boldsymbol{f}_{\mathrm{csb}} \tag{15}$$

$$\cot\phi' = \frac{1}{2} \cdot \frac{a_{\mathrm{v}} + l_{\mathrm{b}}}{h - c - \Delta/2};$$

$$\cot\theta = \frac{a_{\mathrm{v}}}{h - \Delta}; \tag{16}$$

$$T_{\mathrm{i}}' = \frac{P_{\mathrm{max}}}{2} \cdot \cot\phi'$$

where $\Delta = \frac{T_{\mathrm{i}}'}{b\boldsymbol{f}_{\mathrm{cnt}}}$

Equations 15 and 16 can be solved iteratively for Δ and hence P_{max}. The stirrup index SI was only greater than $\mathrm{SI}_{\mathrm{max}}$ in one of the 143 beam tests with stirrups analysed in this paper, (beam V355/3 tested by Lehwalter, 1988), which indicates that the STM is applicable in the majority of practical cases.

Members without vertical shear reinforcement ($\lambda = 1$). In short-span beams with no shear reinforcement, the entire load is transferred from the loading plate to the support through the direct strut (strut I in Figure 1). In this case, analysis of the bottom node gives

$$P = 2\left(l_{\mathrm{b}} \sin^2\theta + c\sin 2\theta\right) b\boldsymbol{f}_{\mathrm{csb}} \tag{17}$$

Consideration of vertical equilibrium and geometry at the top node also gives

$$P = 4\tan\theta\left[d - \left(a - \frac{l_{\mathrm{t}}(2 - n_{\mathrm{lp}})}{4}\right)\tan\theta\right] b\nu\,\boldsymbol{f}_{\mathrm{cd}} \tag{18}$$

The failure load (P) and the strut inclination θ can be calculated by solving Equations 17 and 18.

Step 1: Estimate λ_i and $\cot\theta_i$

Step 2: Calculate β_i

$$\beta_i = \frac{C_1(1 + \cot^2\theta_i) - \lambda_i l_b}{2c\cot\theta_i} > 0 \qquad \text{where} \quad C_1 = \frac{\lambda_i \cdot \sum_1^n T_{Si}}{(1 - \lambda_i) b f_{csb}}$$

Step 3: Calculate tensile forces T_i' and T_d

$$\cot\phi_i' = \frac{\lambda_i(1 - \beta_i)}{\beta_i(1 - \lambda_i)} . \cot\theta_i$$

$$T_i' = \cot\theta_i' \sum_1^n T_{Si} \quad \text{and} \quad T_d = \frac{\lambda}{1 - \lambda_i} . \cot\theta_i \cdot \sum_1^n T_{Si}$$

Step 4: Calculate values for step $i + 1$

$$\lambda_{i+1} = \frac{\cot\theta_i . (h - c\beta_i - C_2) - a_v}{(l_b/2) + (l_t n_{lp}/4)} \qquad \text{where} \quad C_2 = \frac{T_i' + T_d/2}{b f_{cnt}}$$

$$\cot\phi_{i+1}' = \frac{1}{2} . \frac{a_v + (1 + \lambda_{i+1}) l_b}{h - (1 + \beta_i)c - (T_i'/(2b f_{cnt}))}$$

$$\cot\theta_{i+1} = \cot\phi_{i+1}' . \frac{\beta_i (1 - \lambda_{i+1})}{\lambda_{1+1}(1 - \beta_i)}$$

Step 5: Check for convergence

- if $|\lambda_{i+1} - \lambda_i| > tolerance$ and $|\cot\theta_{i+1} - \cot\theta_i| > tolerance$
  go back to step 1 and continue iteration with $\lambda_i = \lambda_{i+1}$ and $\cot\theta_i = \cot\theta_{i+1}$
- otherwise go to step 6

Step 6: Calculate solution

$$\textit{Analysis}: \quad P = \frac{2\sum_1^n T_{Si}}{1 - \lambda_{i+1}} \qquad \text{for } \textit{Design}: \quad A_{sw} = \frac{P(1 - \lambda_{i+1})}{2 f_y} \qquad \text{with} \quad \sum_1^n T_{Si} = \frac{P(1 - \lambda_{i+1})}{2}$$

if $\lambda_{i+1} < 0$ Change section size, f_{cd}, l_t or l_b (stirrups might not yield)

if $\lambda_{i+1} > 1$ No stirrups required (provide minimum quantity of shear reinforcement)

Figure 3. Proposed algorithm for solving simplified strut-and-tie model for short-span beams with stirrups; refer to Figure 2 for notation. Note: i) in STM-EC2, $\mathbf{f}_{csb}$ is taken as 0·6$\nu\mathbf{f}_{cd}$; ii) in STM-Collins, $\mathbf{f}_{csb}$ is obtained iteratively in steps 2–3 using Equation (11); the tensile strain in the tie is obtained from the force $T_i' + T_d$

Influence of aggregate fracture on shear strength

The authors tested two sets of four centrally loaded short-span beams to assess the influence of aggregate fracture on shear strength. The first set of beams are labelled AL0 to AL4 inclusive where A is the series reference, L denotes limestone aggregate and the number of stirrups in each shear span varies between 0 and 4 as indicated. The second set of beams AG0 to AG4 is designated similarly with G denoting gravel aggregate. Figure 4 shows details of the beams and loading arrangement, both of which are fully described elsewhere (Sagaseta, 2008). The beams measured 500 mm high by 135 mm wide and were simply supported over a span of 1320 mm between the centrelines of supports. The flexural reinforcement consisted of two layers of two H25 bars. The effective depth d to the centroid of the flexural reinforcement was 438 mm as shown in Figure 4. The coarse aggregate had a maximum size of 10 mm and was limestone in the AL beams and gravel in the AG beams. The beams were intended to have similar concrete cylinder strengths of around 60 MPa but the concrete delivered by the supplier had cylinder strengths of 68·4 MPa and 80·2 MPa for the AL and AG beams respectively. The cracks passed completely through the limestone aggregate but only through a small proportion of the gravel aggregate.

The loading plate measured 210 × 135 mm on plan. Failure was encouraged to develop in the left hand shear span by making the length of the right-hand bearing plate 200 mm compared with 125 mm in the left-hand span. The increased length of the right-hand bearing plate results in a 20% increase in strength according to the STM or 8% according to the simplified method in Eurocode 2 (Equation 3). Of the eight beams tested, six failed in the left-hand shear span with $a_v/d = 1{\cdot}12$ as expected and only two (AG4, AL2) failed in the right-hand span with $a_v/d = 1{\cdot}04$. The

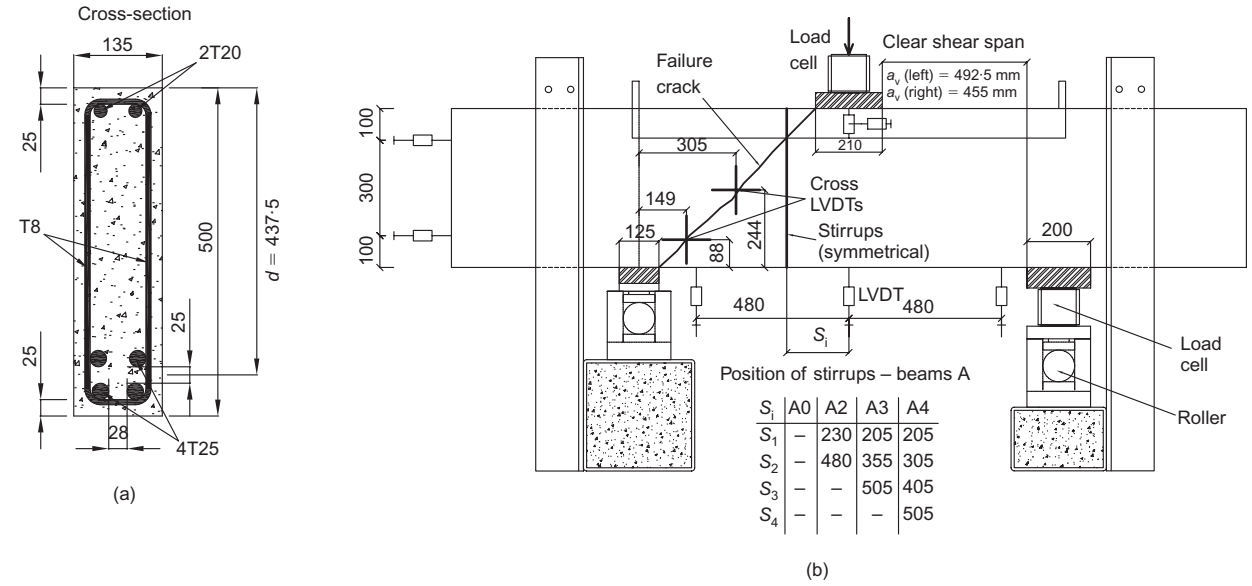

Figure 4. (a) Cross-section of beams A; (b) test arrangement: geometry, position of stirrups, loading plates and instrumentation (LVDTs)

measured and predicted failure loads of the beams are given in Table 1. All of the beams failed in shear but the flexural reinforcement yielded in beams AG3 and AG4. The majority of the beams failed in 'shear compression', which was characterised by crushing of the concrete near the loading plate at failure. The diagonal shear crack ran below the direct strut in these beams and only extended to the inner edges of the plates near failure as shown in Figure 5(a).

The relative opening and sliding displacements of the main shear crack were monitored during the test by means of crosses made up of transducers (linear variable displacement transducers (LVDTs)) and Demec targets. The crack displacements from each method agreed well with each other and visual measurements of crack width (Sagaseta, 2008). A parallel set of push-off tests were carried out using the same types of aggregate as in the beams (Sagaseta, 2008). The push-off specimens were pre-cracked before loading. Despite the aggregate fracturing, shear stresses as high as 5·6 MPa were measured in the limestone push-off specimens with similar concrete strengths and shear reinforcement ratios to the AL beams. Figure 6 shows the relative crack opening (w) and sliding (s) displacements in the beams tested in this program. The average ratio between w and s at the main shear crack was $w/s = 3$ compared with $w/s = 0{\cdot}5$ in the push-off tests implying that crack opening was dominant in the short-beam tests.

The difference in aggregate types does not seem to have affected the crack patterns or strengths of the beams. For example, beam AG0 had a higher concrete

Table 1. Summary of short beams tested by the authors (beams A)

Beam	Critical a_v/d	ρ_v: %	SI	V_{test}: kN	P_{calc}/P_{test} (STM–Eurocode 2)	P_{calc}/P_{test} (Eurocode 2)	P_{calc}/P_{test} (NLFEA)‡
AG0	1·12	0	0	326	1·27	0·53	0·95
AG2	1·12	0·22	0·020	563	0·82	0·35	0·90
AG3*	1·12	0·34	0·031	655	0·73	0·45	0·82
AG4*	1·04	0·45	0·041	707	0·71	0·56	0·53†
AL0	1·12	0	0	366	1·04	0·45	0·80
AL2	1·04	0·22	0·024	532	0·79	0·37	0·98
AL3	1·12	0·34	0·036	481	0·92	0·61	0·97
AL4	1·12	0·45	0·048	602	0·77	0·65	0·83
				Mean	0·88	0·50	0·84
				SD	0·19	0·11	0·14
				COV%	21·6	21·9	17·3

Notes: $\boldsymbol{f}_y$(stirrups) = 550 MPa, $\boldsymbol{f}_y$ (longitudinal) = 580 MPa
* Flexure reinforcement started to yield at failure
$\rho_v = A_{sw}/(ab) \times 100$
† The analysis stopped prematurely
‡ NLFEA – non-linear finite-element analyses

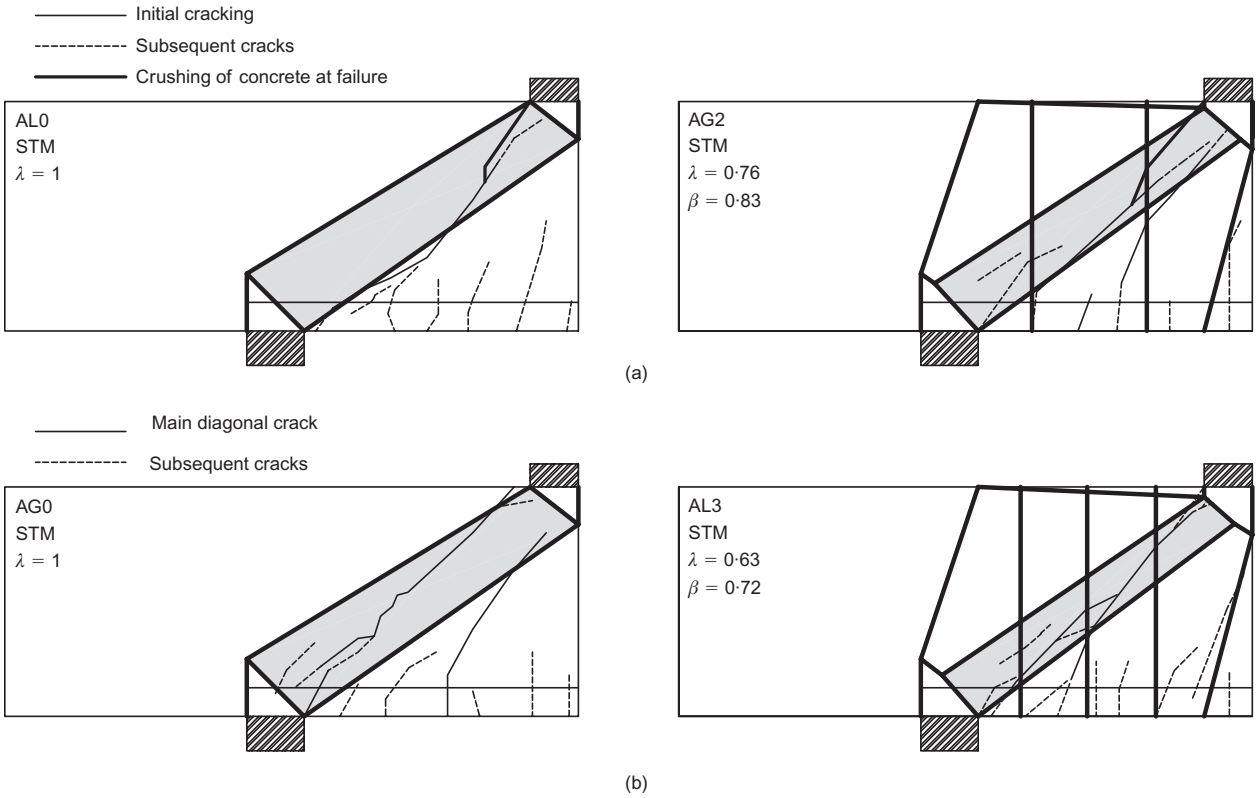

Figure 5. Superimposed crack pattern and strut-and-tie model in beams failing in: (a) shear compression ((AL0, AG2) (AL2, AL4, AG3, AG4 similar but not shown); and (b) shear proper (AG0, AL3)

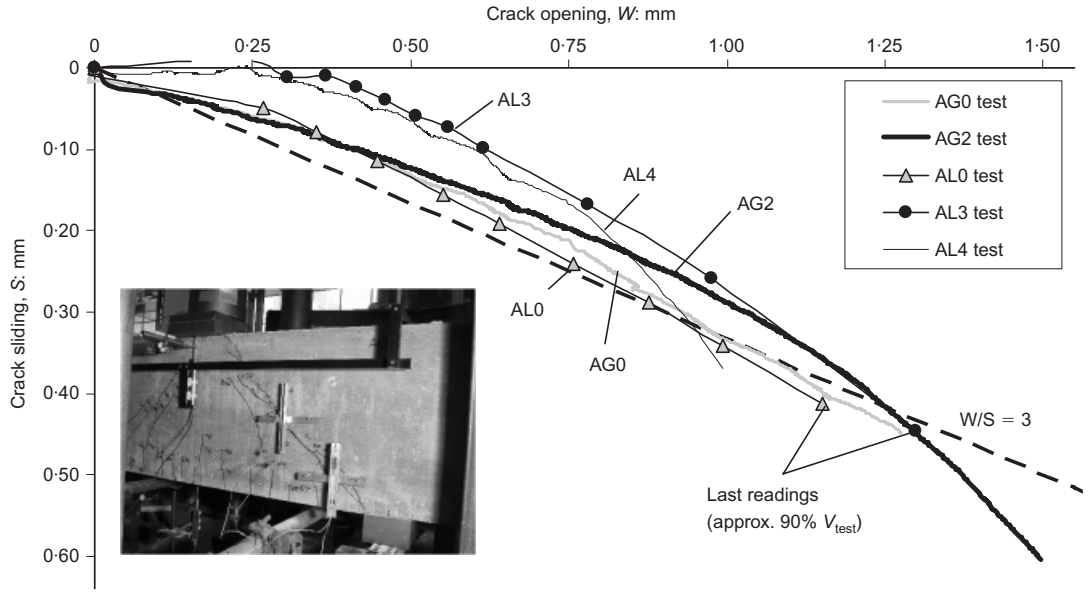

Figure 6. Relative crack displacements measured at mid-height of critical shear crack in beams tested by the authors. Measurements are shown for all specimens until peak load, except for AL0 and AL3 (last readings were taken at 89% and 94% of V_{test} respectively)

strength and rougher crack surface than AL0 but failed at a lower load. Higher shear stresses are likely to have developed along the main shear crack in beam AG0 than in AL0, since the crack opening and sliding displacements were similar in each beam (see Figure 6). The relatively low strength of beam AG0 seems to be related to the orientation of the shear crack which ran diagonally between the corners of the strut from first cracking, as shown in Figure 5(b). This type of failure is usually designated as 'shear-proper'. Similar differences in failure mode were observed in beams AL2 and AL3 with two and three stirrups respectively. Beam AL3 failed in shear-proper (see Figure 5(b)) at a lower load than AL2 which failed in shear compression (see

Figure 5(a)). It appears that the strength of the direct strut depends on the position and orientation of the shear crack which varies randomly. The consequent variation in the strength of the direct strut would appear to explain the large scatter apparent in data from short-span beam tests, which is greatest for beams without stirrups where the contribution of the direct strut is greatest. These observations suggest that

(*a*) random variations in the orientation of the diagonal crack have a greater effect on shear strength than variations in local crack roughness owing to aggregate fracture
(*b*) the influence of aggregate interlock is likely to be greatest in beams without stirrups that fail in shear-proper.

Sagaseta (2008) obtained reasonable predictions for the shear strength of short-span beams which fail in shear-proper, for example beam AG0, by calculating the strength of the direct strut in terms of shear friction along the crack. The drawback of this approach is that the predictions are highly dependent on the values assumed for crack inclination, friction and cohesion, all of which are difficult to assess unless experimental data are available. The method also underestimates the strength of beams which fail in shear compression. Therefore, the adoption of a constant strength reduction factor for the concrete seems more suitable for design.

Comparison between STM and NLFEA predictions

Non-linear finite-element analyses (NLFEA) were carried out on the beams tested in this project, using plane stress elements to check the geometry and stress distributions assumed in the STM. The NLFEA was performed with the commercial package DIANA v9 (DIANA, 2005) using the multi-directional fixed crack model which is based on strain decomposition and combines plasticity for compression (Drucker–Prager) and smeared cracking for tension. Reinforcement is modelled as embedded elements with a Von Mises perfectly plastic material. Table 1 gives the failure loads calculated with NLFEA using the material properties summarised in Table 2.

The orientation of the cracks along the direct strut, stiffness of the beam and the predicted failure load were found to be sensitive to the concrete tensile strength adopted in the analysis. The results were poor if the measured concrete tensile strengths from Brazilian tests were used in the analysis. Much better results were obtained when the concrete tensile strength was taken as $\boldsymbol{f}_{ct} = 0{\cdot}33(\boldsymbol{f}'_c)^{0{\cdot}5}$ in accordance with the recommendations of Bresler and Scordelis (1963), which provide lower values of $\boldsymbol{f}_{ct}$ than the Brazilian tests. The comparison between the measured and predicted failure loads was better than expected since the concrete strength was not reduced in the NLFEA to account for transverse strains. However, the predicted failure load was found to be sensitive to variations in the strength of the highly stressed elements adjacent to the loading plate shown in Figure 7(a). The strength of these elements is increased by the confinement provided by the loading plate, which is not modelled in the two-dimensional model used by the authors. The strength of

Table 2. Parameters applied in the non-linear finite element analysis

Concrete	AG	AL	Steel	Stirrups and plates	Long. Reinf.
E_c: MPa	42 600	35 000	E_s: GPa	200	200
ν	0·2	0·2	ν	0·3	0·3
$\boldsymbol{f}_{ct}$: MPa	2·95	2·70	$\boldsymbol{f}_y$: MPa	550	580
G_f : N/mm	0·113	0·101			
$\boldsymbol{f}'_c$: MPa	80·2	68·4			

Notes: Concrete – multi-directional fixed crack model: threshold angle $\alpha = 60°$, shear retention factor $\beta = 0{\cdot}1$, Drucker–Prager plasticity ($\Phi = \Psi = 10°$) with parabolic hard strain stiffening; $\boldsymbol{f}_{ct}$ according to Bresler and Scordelis (1963)
Steel – Perfect plasticity (Von Mises)

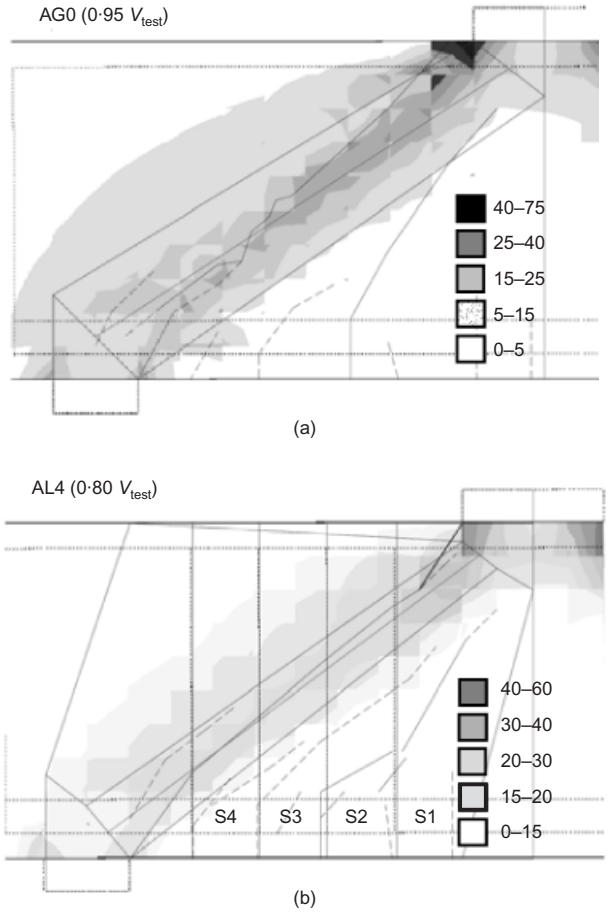

Figure 7. Principal compressive stresses (in MPa) predicted in the NLFEA and superimposition of experimental crack pattern and STM: (a) beam AG0; and (b) beam AL4

beam AG4 was underestimated since the authors were unable to find a converged solution.

The STM assumes a uniform stress distribution under the loading plates whereas the NLFEA shows stress concentrations at the edge of the loading plate, as shown in Figure 7. The stress concentrations in the FE model depend on the stiffness assumed for the loading platen and the cracking model adopted for concrete. The stress concentration near the edge of the loading plate in the NLFEA resulted in a slightly steeper strut than predicted in the STM as shown in Figure 7(a). Even so, the numerical predictions agreed well with those of the STM for beams such as AL4, where the orientations of the direct strut were similar in both the STM and NLFEA (see Figure 7(b)). The sizes of the nodes were also similar in the NLFEA and STM for beam AL4.

The NLFEA predicted that the shear reinforcement yielded prior to failure, as measured and assumed in the STM. The results shown in Figure 8 for beams AG3 and AL3 correspond to the stirrups in the critical span ($a_v/d = 1{\cdot}12$). The NLFEA predicted higher stresses in the stirrups at the intersection with the diagonal crack as measured. The strains derived from the Demec gauge readings are generally larger than measured with the strain gauges or predicted in the NLFEA. This is somewhat surprising but appears to be related to the strain gauges not coinciding with cracks, more than

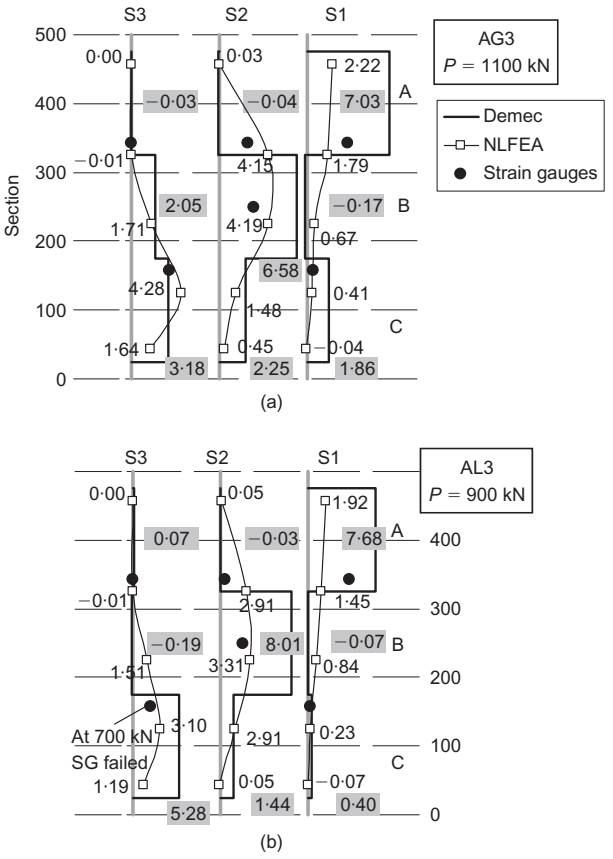

Figure 8. Variation of strains (‰) at different heights of the stirrup: (a) beam AG3; and (b) beam AL3

one crack forming within the Demec gauge lengths and spalling of the cover zone. The tensile strains in the flexural reinforcement of beam AG0 were similar at the inner edge of support and beam centreline respectively as predicted in the STM. The gradient in the tensile strain along the flexural reinforcement predicted by the STM model agrees well with the measured strains and NLFEA predictions for beams AL3 and AG3 as shown in Figure 9.

Assessment of design methods for beams with stirrups

The accuracy of the STM, the modified truss and the simplified design methods in MC90 and Eurocode 2 were assessed with a database of 143 beams that failed

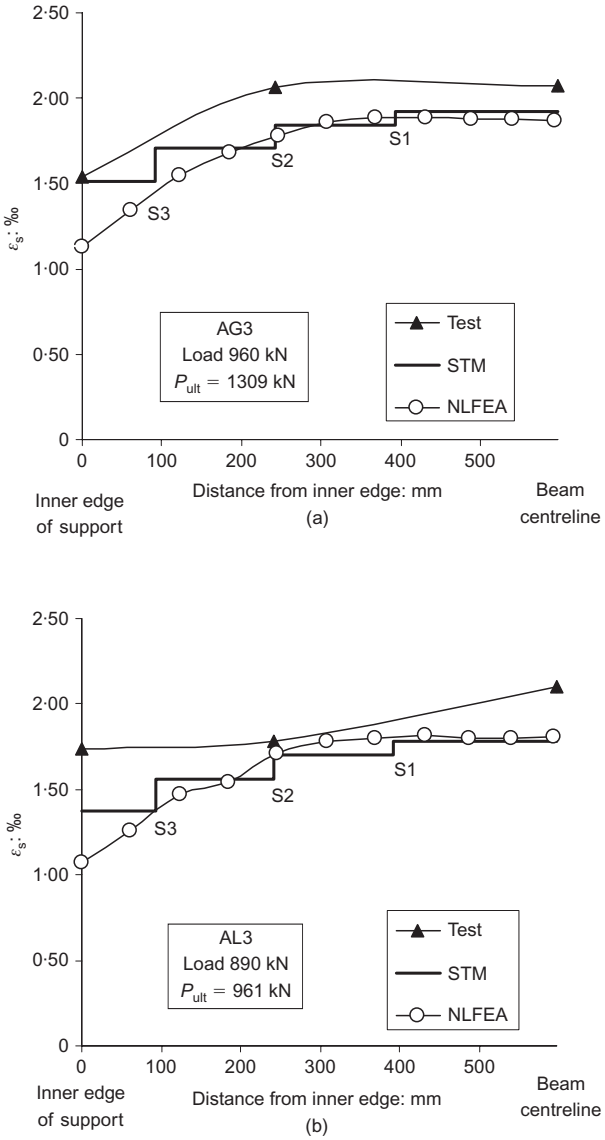

Figure 9. Comparison of predicted and experimental gradient of tensile strains along the flexural reinforcement from the inner edge of the support to the centre of the beam: (a) beam AG3; and (b) beam AL3

in shear (Clark 1951; Kong *et al.*, 1970; Kong and Rangan, 1998; Lehwalter, 1988; Rawdon de Paiva and Siess, 1965; Regan, 1971; Sagaseta, 2008; Sarsam and Al-Musawi, 1992; Tan *et al.*, 1995, 1997; Vollum and Tay, 2001; Zhang and Tan, 2007). The clear shear span to effective depth ratio (a_v/d) of the beams analysed varied between 0·25 and 2·4. Table 3 gives details of the 47 beams with a_v/d ratios between 1 and 2. The top and bottom bearing plates were of equal length in the majority of the beams (i.e. $l_t.n_{lp}/2 = l_b$). The material factors of safety were taken as 1·0 in all the analyses. No significant differences were found be-

Table 3. Experimental data for short-span beams with stirrups ($a_v/d = 1-2$)

Tests with stirrups (a_v/d: 1–2)									P_{calc}/P_{test}				
Ref.	Beam	a_v/d	h: mm	d: mm	b: mm	f'_c: MPa	SI	P_{test}: kN	MC90	V_d+V_s	Eurocode 2	STM–Eurocode 2	STM–Collins
1	V3511/3	1·25	600	560	250	17	0·154	970	0·73	1·19	1·30	–	–
2	J6	1·57	305	272	152	32	0·046	292	0·32	0·89	0·58	0·87	0·71
	J10	1·10	305	272	152	32	0·031	272	0·30	0·99	0·66	1·05	0·99
	J17	1·10	305	272	152	40	0·054	530	0·34	0·74	0·68	0·72	0·70
	J19	1·10	305	272	152	35	0·028	366	0·22	0·75	0·51	0·84	0·78
	J20	1·10	305	272	152	35	0·028	320	0·25	0·86	0·58	0·97	0·91
	J8	1·68	305	254	152	34	0·029	370	0·16	0·59	0·34	0·81	0·64
3	E-1·62-3·23	1·30	500	463	110	51	0·042	440	0·45	0·96	0·83	1·06	0·92
4	III-2N/1·50	1·41	500	443	110	78	0·052	670	0·53	1·00	0·94	1·10	1·08
	III-2S/1·50	1·41	500	443	110	78	0·066	800	0·56	0·98	0·99	0·99	1·00
5	5	1·14	200	180	100	44	0·058	220	0·40	0·92	0·81	0·83	0·84
	6	1·14	200	180	100	44	0·115	250	0·70	1·21	1·42	0·87	0·93
6	B1-1	1·72	457	390	203	23	0·065	558	0·35	0·87	0·59	0·83	0·71
	B1-2	1·72	457	390	203	25	0·060	513	0·38	0·96	0·64	0·95	0·81
	B1-3	1·72	457	390	203	24	0·064	570	0·34	0·86	0·57	0·82	0·70
	B1-4	1·72	457	390	203	23	0·065	536	0·36	0·91	0·61	0·86	0·74
	B1-5	1·72	457	390	203	25	0·062	483	0·40	1·02	0·68	0·99	0·84
	B2-1	1·72	457	390	203	23	0·109	602	0·54	1·12	0·91	0·90	0·81
	B2-2	1·72	457	390	203	26	0·096	644	0·50	1·06	0·85	0·90	0·81
	B2-3	1·72	457	390	203	25	0·101	670	0·49	1·01	0·81	0·84	0·76
	B6-1	1·72	457	390	203	42	0·036	759	0·26	0·70	0·43	0·91	0·72
	C1-1	1·33	457	390	203	26	0·039	555	0·29	0·83	0·51	0·95	0·84
	C1-2	1·33	457	390	203	26	0·038	622	0·26	0·74	0·45	0·86	0·76
	C1-3	1·33	457	390	203	24	0·042	492	0·33	0·92	0·57	1·02	0·90
	C1-4	1·33	457	390	203	29	0·035	572	0·28	0·83	0·50	1·01	0·88
	C2-1	1·33	457	390	203	24	0·064	580	0·42	0·94	0·73	0·92	0·85
	C2-2	1·33	457	390	203	25	0·061	602	0·40	0·92	0·70	0·92	0·84
	C2-4	1·33	457	390	203	27	0·056	576	0·42	0·97	0·73	1·01	0·92
	C3-1	1·33	457	390	203	14	0·072	447	0·36	0·92	0·63	0·75	0·72
	C3-2	1·33	457	390	203	14	0·073	401	0·41	1·02	0·70	0·83	0·79
	C3-3	1·33	457	390	203	14	0·073	376	0·43	1·09	0·75	0·89	0·85
	C4-1	1·33	457	390	203	24	0·041	619	0·26	0·74	0·46	0·82	0·76
	C6-2	1·33	457	390	203	45	0·022	848	0·19	0·61	0·39	0·94	0·84
	C6-3	1·33	457	390	203	45	0·023	870	0·19	0·59	0·38	0·91	0·81
	C6-4	1·33	457	390	203	48	0·021	857	0·19	0·61	0·39	0·97	0·86
	D1-6	1·66	381	314	152	28	0·029	349	0·19	0·68	0·41	0·95	0·73
	D1-7	1·66	381	314	152	28	0·029	358	0·18	0·66	0·40	0·94	0·72
	D1-8	1·66	381	314	152	28	0·029	372	0·18	0·64	0·38	0·90	0·69
	E1-2	1·74	381	314	152	30	0·080	444	0·42	0·95	0·73	0·96	0·82
7	S5-4	1·64	350	292	250	89	0·011	953	0·12	0·53	0·35	1·14	0·83
	S5-5	1·40	350	292	250	89	0·008	1147	0·09	0·45	0·34	1·04	0·81
8	AG2	1·13	500	438	135	80	0·020	1126	0·18	0·50	0·35	0·82	0·84
	AG3	1·13	500	438	135	80	0·031	1309	0·23	0·52	0·45	0·73	0·77
	AG4	1·13	500	438	135	80	0·041	1414	0·28	0·56	0·56	0·71	0·75
	AL2	1·13	500	438	135	68	0·024	1064	0·19	0·51	0·37	0·79	0·80
	AL3	1·13	500	438	135	68	0·036	961	0·31	0·68	0·61	0·92	0·95
	AL4	1·13	500	438	135	68	0·048	1204	0·33	0·64	0·65	0·77	0·81
	max.	**1·74**	**600**	**560**	**250**	**89**	**0·154**	**Avg.**	**0·33**	**0·82**	**0·62**	**0·90**	**0·82**
	min.	**1·10**	**200**	**180**	**100**	**14**	**0·008**	**S.D.**	**0·14**	**0·20**	**0·23**	**0·10**	**0·09**
	tests	47						**Cov.**	**0·42**	**0·24**	**0·37**	**0·11**	**0·11**

References: (1) Lehwalter, 1988; (2) Regan, 1971; (3) Tan *et al.*, 1995; (4) Tan *et al.*, 1997; (5) Vollum and Tay, 2001; (6) Clark, 1951; (7) Kong and Rangan, 1998; (8) Sagaseta, 2008. Avg. = average, S.D. = standard deviation and Cov. = covariance

tween the predictions of the simplified STM solution procedure described in Figure 3 and the more general solution procedure described in the text which accounts for the actual position of the stirrups. Results are given for the STM with the strength of the direct strut calculated in accordance with Eurocode 2 (STM–Eurocode 2) and the recommendations of Collins and Mitchell (1991) (STM–Collins). The concrete contribution (V_d) was taken as $(2d/a_v)V_c$ in the modified truss model where V_c was calculated with Equation 1.

Figure 10 shows that the STM is the only method to accurately account for the influence of the stirrup index *SI* on shear strength. Figure 11 show that the STM–Collins predicts the influence of a_v/d most realistically and that the STM–Eurocode 2 tends to give unsafe predictions when $a_v/d > 2$. When $a_v/d > 2$ the strength should be taken as the greatest of the values given by sectional analysis and STM–Collins. Table 3 shows that the STM was the most accurate of the methods considered for beams with stirrups and $1 < a_v/d < 2$. Figure 12 shows the proportion of shear force taken by the direct strut (λ) in the STM decreases with increasing SI, which is not the case for the modified truss, Eurocode 2 or MC90 where P_{calc}/P_{test} varies significantly with stirrup index (see Figures 10(a)–(c)). This explains why the coefficients of variation in P_{calc}/P_{test} in Table 3 are significantly greater for Eurocode 2 (37·7%) and the modified truss model ($V_d + V_s$) (24·1%) than for the STM (10%).

Predictions for members without shear reinforcement

A total of 104 short-span beams (Cheng *et al.*, 2001; Clark, 1951; de Cossio and Siess, 1960; Kong *et al.*, 1970; Lehwalter, 1988; Leonhardt and Walter, 1964; Mathey and Watsein, 1963; Moody *et al.*, 1954, Oh and Shin, 2001; Placas, 1969; Reyes de Ortiz, 1993; Sagaseta, 2008; Smith and Vantsiotis, 1982; Tan and Lu, 1999; Tan *et al.*, 1997; Vollum and Tay, 2001; Walraven and Lehwalter, 1994; Zhang and Tan, 2007) without stirrups were analysed with the STM and the sectional design method in Eurocode 2 with partial factors γ_c and γ_s equal to 1·0. The Eurocode 2 shear capacity was taken as $V_{calc} = (2d/a_v)V_{Rdc}$ where V_{Rdc} is given by Equation 1 and $2d/a_v \geqslant 1$. Table 4 gives detailed results for the 67 beams with $1 < a_v/d < 2$. All of the results are presented in Figure 13, which shows that the accuracy of both methods is relatively independent of a_v/d but STM–Eurocode 2 gives significantly greater values for P_{calc}/P_{test}. Table 4 shows that STM–Eurocode 2 predicts the mean strength of the

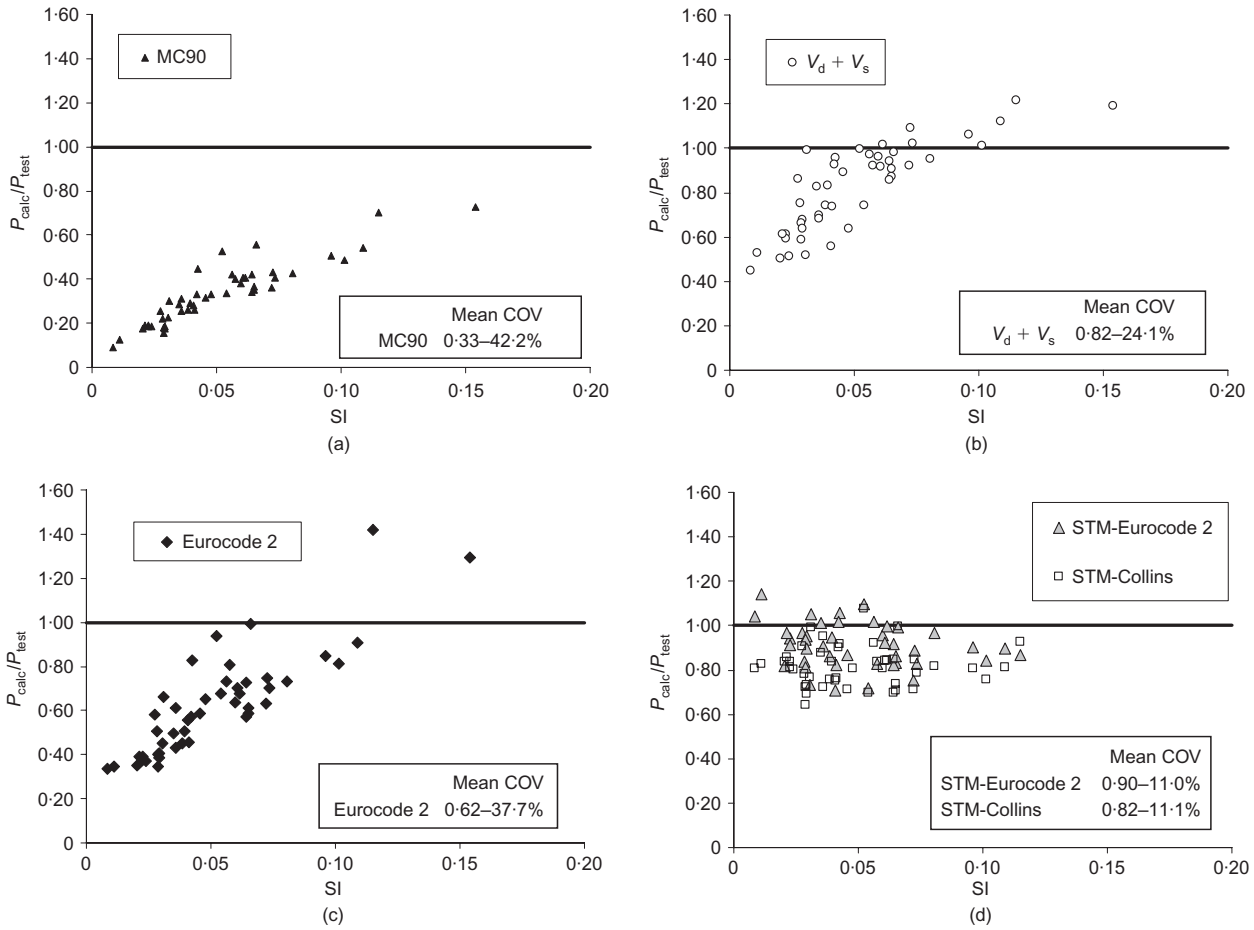

Figure 10. Performance of design methods of short span beams ($1 < a_v/d < 2$) with stirrups: (a) MC90 formula; (b) standard truss ($V_d + V_s$) method; (c) Eurocode 2 simplified method; and (d) proposed strut-and-tie model (STM). COV – coefficients of variation

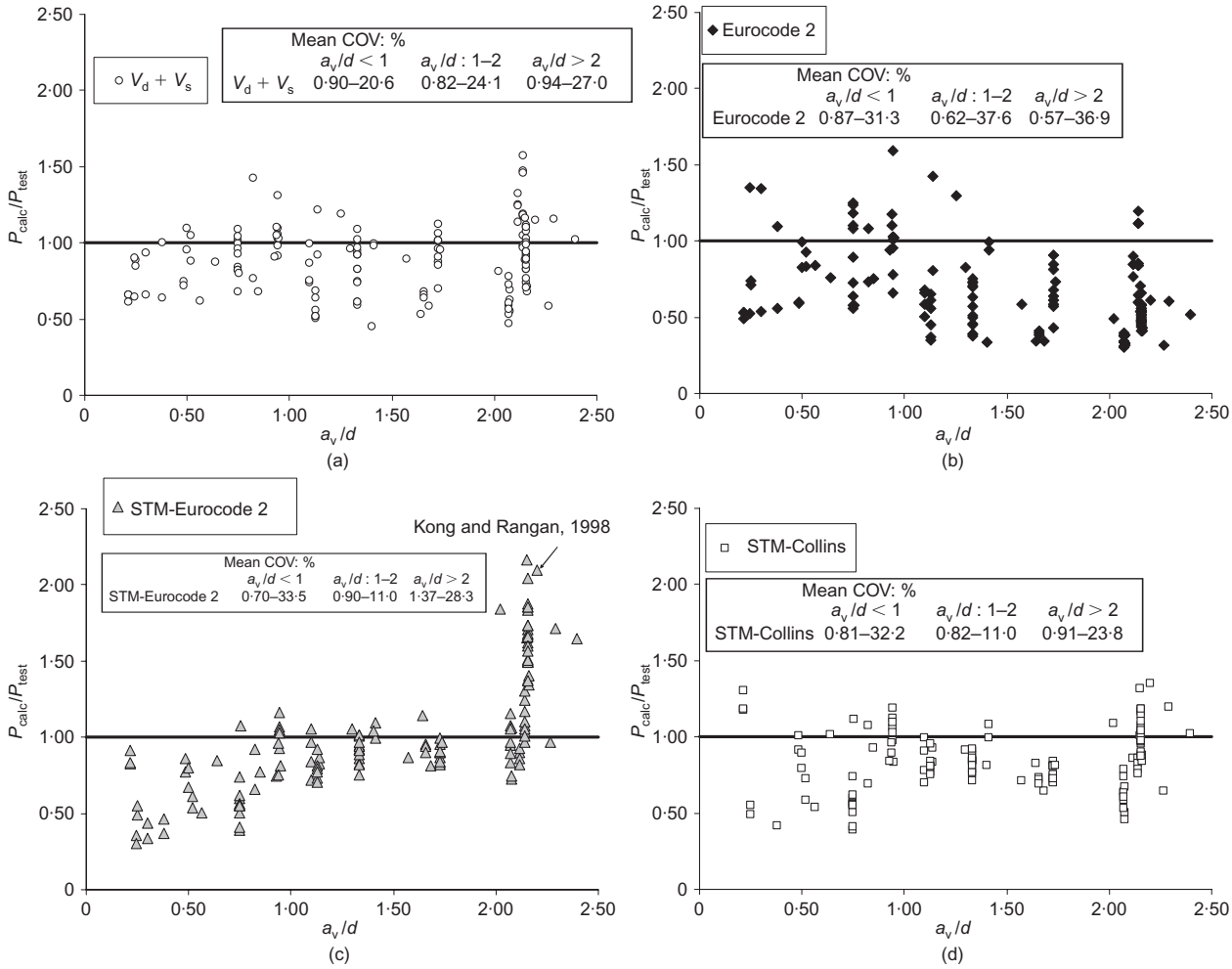

Figure 11. Influence of the a_v/d ratio in the predictions for different design methods (short span beams with stirrups): (a) standard truss ($V_d + V_s$) method; (b) Eurocode 2 simplified method; (c) strut-and-tie model (STM-Eurocode 2); and (d) strut-and-tie model (STM-Collins)

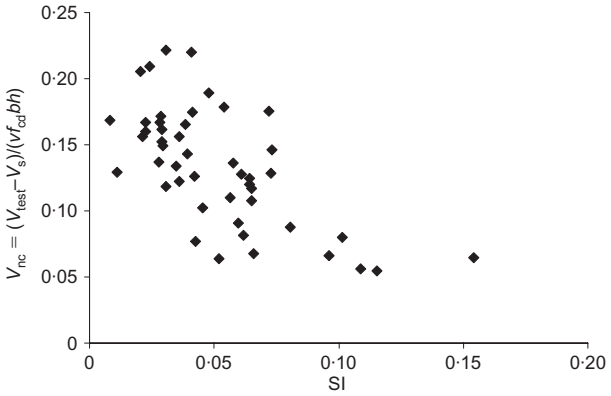

Figure 12. Variation of normalised shear force carried by the direct strut ($V_{nc} = (V_{test}-V_s)/(nf_{cd}bh)$) with the stirrup index (SI); beams with $1 < a_v/d < 2$ (refer to Table 3)

beams with $1 < a_v/d < 2$ most accurately but overestimates the strength of a significant number of beams. Table 4 also shows that STM–Collins tends to give safe predictions for the beams with strengths that are overestimated by STM–Eurocode 2.

Tables 3 and 4 give coefficients of variation (COV) for each design method for beams with and without stirrups and $1 < a_v/d < 2$. For example, the COV for STM–Eurocode 2 was 11% for beams with shear reinforcement and 26% for beams without stirrups. Comparison of the strengths of notionally identical beams tested by Clark (1951), Kong and Rangan (1998), Vollum and Tay (2001) among others suggest that a significant proportion of the greater scatter in P_{calc}/P_{test} for beams with little or no shear reinforcement is inherent in the test data.

Design recommendations

Comparison of Figures 11(c) and 11(d) suggests that the proposed STM is most reliable when the concrete strength in the direct strut is calculated in accordance with Equation 11 (Collins and Mitchell, 1991). This is further illustrated in Figures 14(a)–(c), which compare the predictions of various design methods, including STM–Eurocode 2 and STM–Collins, with test data

Table 4. Summary of database of members without stirrups (a_v/d = 1–2)

Tests without stirrups (a_v/d: 1–2)									P_{calc}/P_{test}			
Ref.	Beam	a_v/d	*h:* mm	*d:* mm	*b*: mm	f'_c: MPa	*ρ:* %	P_{test}: kN	STM–Eurocode 2	STM–Collins	Eurocode 2	BS 8110
9	BI-1	1·29	457	403	203	26	3·05	626	0·64	0·59	0·46	0·50
	BI-2	1·29	457	403	203	23	3·05	621	0·59	0·54	0·45	0·49
	BII-3	1·29	457	403	203	22	1·88	524	0·67	0·57	0·51	0·49
	BII-4	1·29	457	403	203	27	1·88	626	0·67	0·56	0·46	0·43
	BIII-5	1·29	457	403	203	26	1·85	577	0·70	0·59	0·49	0·46
	BIII-6	1·29	457	403	203	26	1·85	581	0·70	0·59	0·49	0·46
	BIV-7	1·29	457	403	203	25	1·86	582	0·66	0·56	0·48	0·45
	BIV-8	1·29	457	403	203	25	1·86	608	0·65	0·55	0·46	0·44
	BV-9	1·29	457	403	203	24	1·16	448	0·83	0·64	0·52	0·49
	BV-10	1·29	457	403	203	27	1·16	537	0·79	0·60	0·46	0·43
	BVI-11	1·29	457	403	203	26	1·17	448	0·90	0·69	0·54	0·51
	BVI-12	1·29	457	403	203	26	1·17	537	0·75	0·58	0·45	0·43
	BV-13	1·29	457	403	203	23	0·75	445	0·81	0·57	0·45	0·43
	BV14	1·29	457	403	203	27	0·75	448	0·94	0·64	0·47	0·45
	BVI-15	1·29	457	403	203	26	0·75	359	1·13	0·77	0·58	0·55
	BVI-16	1·29	457	403	203	23	0·75	377	0·97	0·68	0·53	0·51
10	III-24a	1·14	610	533	178	18	2·72	592	0·71	0·61	0·54	0·56
	III-24b	1·14	610	533	178	21	2·72	605	0·79	0·68	0·55	0·57
	III-25a	1·14	610	533	178	25	3·46	534	1·05	0·92	0·66	0·71
	III-25b	1·14	610	533	178	18	3·46	578	0·71	0·63	0·54	0·58
	III-26a	1·14	610	533	178	22	4·25	841	0·60	0·54	0·40	0·43
	III-26b	1·14	610	533	178	21	4·25	792	0·61	0·55	0·42	0·45
	III-27a	1·14	610	533	178	22	2·72	694	0·72	0·61	0·49	0·50
	III-27b	1·14	610	533	178	23	2·72	712	0·74	0·63	0·49	0·50
	III-28a	1·14	610	533	178	24	3·46	605	0·89	0·78	0·58	0·62
	III-28b	1·14	610	533	178	23	3·46	681	0·76	0·67	0·51	0·54
	III-29a	1·14	610	533	178	22	4·25	778	0·65	0·59	0·44	0·47
	III-29b	1·14	610	533	178	25	4·25	872	0·65	0·59	0·41	0·44
11	V311	1·25	1000	930	250	16	1·69	735	0·78	0·71	0·80	0·72
	V321	1·25	1000	930	250	16	1·69	778	0·73	0·67	0·75	0·67
	V322	1·25	1000	930	250	14	1·69	752	0·68	0·63	0·75	0·67
	V811	1·25	200	160	250	19	1·90	281	0·81	0·58	0·54	0·55
12	2	1·10	320	270	190	21	2·07	531	0·52	0·43	0·41	0·40
13	R4	1·99	305	272	152	34	1·46	302	0·51	0·29	0·34	0·33
	R5	1·99	305	272	152	34	0·97	169	0·92	0·48	0·53	0·51
	R6	1·99	305	272	152	34	1·46	249	0·63	0·35	0·41	0·40
14	1	1·14	200	180	100	44	2·23	137	1·05	0·95	0·74	0·76
	2	1·14	200	180	100	44	2·23	201	0·71	0·65	0·50	0·52
	3	1·14	200	180	100	44	1·26	145	0·99	0·79	0·60	0·59
	4	1·28	200	160	100	44	2·51	161	1·19	0·88	0·50	0·55
	7	1·14	200	180	100	25	2·23	135	0·66	0·61	0·62	0·64
	8	1·14	200	180	100	25	2·23	165	0·54	0·50	0·51	0·52
	9	1·14	200	180	100	25	2·23	178	0·50	0·46	0·47	0·48
	10	1·21	200	180	100	25	2·23	180	0·39	0·38	0·44	0·45
	11	1·21	200	180	100	25	2·23	134	0·52	0·51	0·59	0·61
	12	1·21	200	180	100	25	2·23	133	0·53	0·51	0·59	0·61
15	1	1·10	400	363	150	51	1·80	560	1·03	0·83	0·50	0·48
	2	1·24	400	363	150	36	1·80	440	0·75	0·63	0·50	0·48
	3	1·38	400	326	150	32	2·06	310	0·89	0·68	0·59	0·57
	3B	1·38	400	326	150	49	2·06	580	0·67	0·51	0·36	0·35
	4	1·38	400	326	150	33	2·06	490	0·84	0·59	0·38	0·36
16	0C0-50	1·16	356	305	102	21	1·93	232	0·69	0·58	0·51	0·49
	0B0-49	1·16	356	305	102	22	1·93	298	0·56	0·47	0·41	0·39
	0D0-47	1·75	356	305	102	20	1·93	148	0·75	0·47	0·53	0·50
17	1-500/1·5	1·46	500	444	140	42	2·60	680	0·60	0·48	0·33	0·34
	2-1000/1·5	1·53	1000	884	140	39	2·60	940	0·78	0·63	0·39	0·38
	3-1400/1·5	1·55	1400	1243	140	44	2·60	1380	0·76	0·62	0·36	0·35
	4-1750/1·5	1·56	1750	1559	140	43	2·60	940	1·32	1·03	0·64	0·60
18	III-1/1·50	1·41	500	443	110	78	2·58	370	1·34	1·14	0·60	0·62

(*continued*)

Table 4. (continued)

Tests without stirrups (a_v/d: 1–2)									P_{calc}/P_{test}			
Ref.	Beam	a_v/d	h: mm	d: mm	b: mm	f'_c: MPa	ρ: %	P_{test}: kN	STM–Eurocode 2	STM–Collins	Eurocode 2	BS 8110
19	B0-1	1·72	457	390	203	24	0·98	242	0·98	0·80	0·67	0·63
	B0-2	1·72	457	390	203	24	0·98	188	1·26	1·04	0·86	0·82
	B0-3	1·72	457	390	203	24	0·98	256	0·92	0·76	0·63	0·60
	C0-1	1·33	457	390	203	25	0·98	349	0·85	0·85	0·61	0·58
	C0-3	1·33	457	390	203	24	0·98	334	0·89	0·86	0·63	0·59
20	L-1	1·41	305	252	152	21	3·36	232	0·90	0·58	0·56	0·61
21	AG0	1·12	500	438	135	80	3·33	652	1·27	1·33	0·53	0·57
	AL0	1·12	500	438	135	68	3·33	731	1·04	1·05	0·45	0·49
	max.	**1·99**	**1750**	**1559**	**250**	**80**	**4·25**	**Avg.**	**0·79**	**0·65**	**0·52**	**0·52**
	min.	**1·10**	**200**	**160**	**100**	**14**	**0·75**	**S.D.**	**0·21**	**0·19**	**0·11**	**0·10**
	tests	**67**						**Cov.**	**0·26**	**0·28**	**0·21**	**0·20**

References: (9) Mathey and Watsein, 1963; (10) Moody *et al.*, 1954; (11) Lehwalter, 1988; (12) Leonhardt and Walter, 1964, (13) Placas, 1969; (14) Vollum and Tay, 2001; (15) Reyes de Ortiz, 1993; (16) Smith and Vantsiotis, 1982; (17) Cheng *et al.*, 2001; (18) Tan *et al.*, 1997; (19) Clark, 1951; (20) de Cossio and Siess, 1960; (21) Sagaseta, 2008. Avg. = average, S.D. = standard deviation and Cov. = covariance

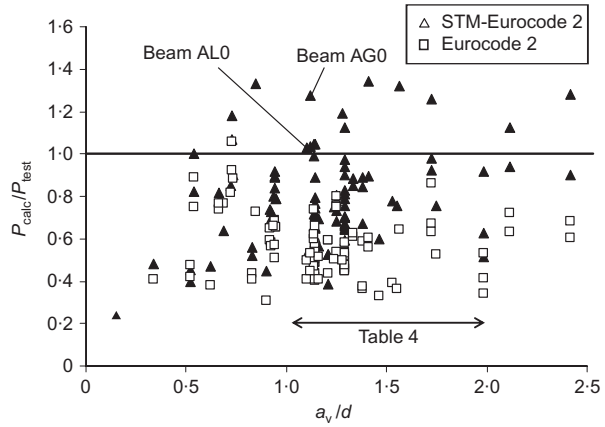

Figure 13. Influence of a_v/d on performance of STM-Eurocode 2 and Eurocode 2 methods for short span beams without stirrups; data from Clark (1951), Moody et al. (1954), de Cossio and Siess (1960), Leonhardt and Walter (1964), Mathey and Watsein (1963), Placas (1969), Kong et al. (1970), Smith and Vantsiotis (1982), Lehwalter (1988), Reyes de Ortiz (1993), Walraven and Lehwalter (1994), Tan et al. (1997), Tan and Lu (1999), Cheng et al. (2001), Oh and Shin (2001), Vollum and Tay (2001), Zhang and Tan (2007), Sagaseta (2008) (refer to Table 4 for tests with $1 < a_v/d < 2$)

from Kong and Rangan (1998) for beams in which the only parameters varied were (*a*) the shear span, (*b*) the stirrup index and (*c*) the area of flexural reinforcement. All the beams of Kong and Rangan (1998) shown in Figure 14 failed in shear unless noted otherwise. Figure 14 shows (*a*) shear strengths calculated assuming the flexural reinforcement remained elastic and (*b*) the shear force corresponding to flexural failure. Comparison of the STM–Eurocode 2 and V_{flex} lines with the test data in Figures 14(a)–(c) shows that the STM–Eurocode 2 incorrectly predicts the failure mode in a significant number of cases. The STM–Eurocode 2 can significantly overestimate the shear strength of beams with $a_v/d > 1{\cdot}64$ as shown in Figure 14(a). Figure 14(a) also shows that the shear strength calculated with Equation 3 can be (*a*) independent of the shear span for beams with uniform stirrup spacing and (*b*) less than that given by the variable strut inclination method for shear reinforcement in Eurocode 2. Neither of these results is consistent with the test data. Figure 14(a) also shows strengths calculated with the method used in BS 8110 but with V_c given by Equation 1 from Eurocode 2. The method gives conservative results but is more realistic than Equation 3 in Eurocode 2. Figures 14(a)–(c) show that STM–Collins gives reasonable predictions of the affect of varying a_v/d, SI and flexural reinforcement ratio on shear strength. The STM–Collins also has the advantage that the predictions of the STM tend to become progressively safer as a_v/d increases.

Conclusion

This paper presents a strut-and-tie model for short-span beams which is shown to provide more accurate predictions of shear strength than existing simplified design equations. The strength of the direct strut can either be calculated in accordance with Eurocode 2 (STM–Eurocode 2) or in accordance with the recommendations of Collins and Mitchell (1991) (STM–Collins). Analysis of test data shows that STM–Eurocode 2 is valid for $a/d < 2$, where the shear span a is measured between the centres of the bearing plates. The restriction on a/d is unnecessary for STM–Collins since the model becomes progressively more conservative as a_v/d increases above 2. The realism of the STM was investigated with NLFEA for beams tested by the authors. Good agreement was obtained between the strains measured in the shear and longitudinal reinforcement and calculated in the STM and NLFEA. The STM strength predictions were more reliable than those from the NLFEA, which were sensi-

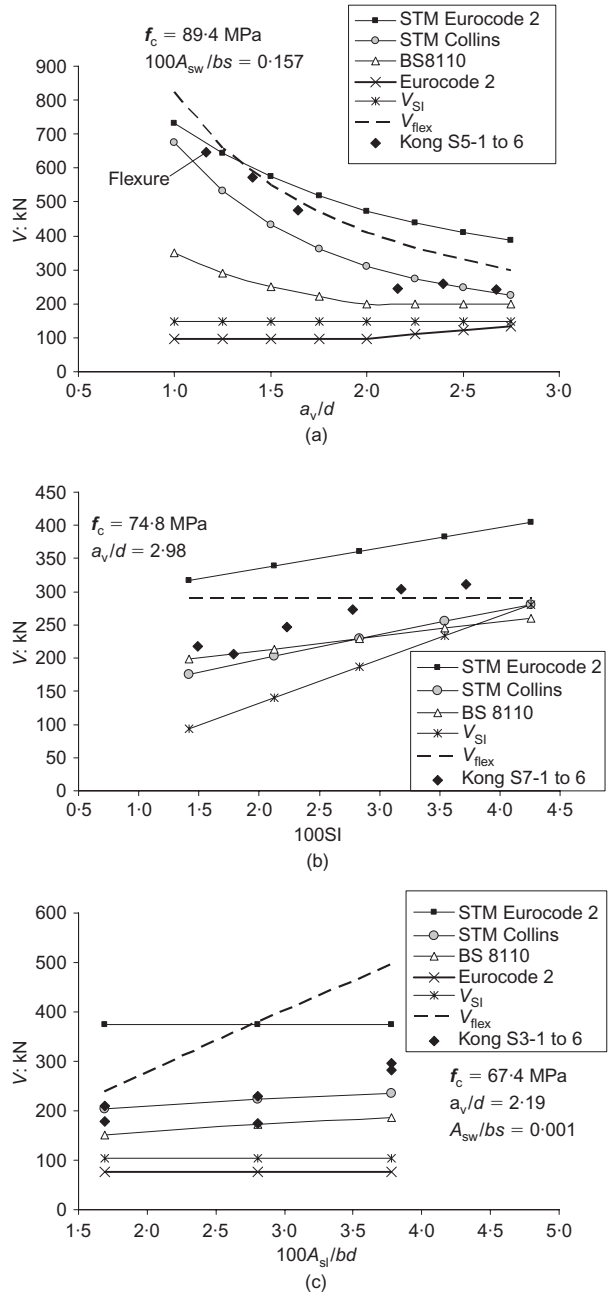

Figure 14. Analysis beams tested by Kong and Rangan (1998) with varying: (a) a_v/d (S5-1 to S5-6); (b) stirrup index (S71-6); (c) flexural reinforcement (S3-1 to 6)

tive to the parameters assumed in the model and subject to convergence difficulties near failure. Analysis of test data showed that the performance of the simplified design method in Eurocode 2 for short-span beams is highly dependent on the stirrup index SI. Similar problems were observed in the MC90 design method, which provides rather conservative results. The proposed STM overcomes this variability in accuracy with SI since the contribution of the direct strut reduces as the SI increases. The STM is most accurate for beams with stirrups and gives the most consistent results when the strength of the direct strut is calculated with the formula of Collins and Mitchell (1991). The scatter in the predictions for beams without stirrups reflects the variability in the test data, which appears to be largely attributable to variations in the orientation of the diagonal shear crack within the direct strut.

The influence of aggregate fracture on the shear strength of short-span beams was investigated experimentally. Analysis of the relative crack displacements and comparison of the predicted and measured failure loads suggests aggregate fracture has little if any influence on the shear strength of short-span beams but more tests are required to confirm this. The orientation of the main diagonal shear crack with respect to the direct strut appears to have a much more significant effect than crack roughness for the specimens tested.

Acknowledgements

The authors would like to acknowledge the financial support of the Fundación Caja Madrid and thank the staff of the Concrete Structures Laboratory at Imperial College London.

References

Bresler B and Scordelis AC (1963) Shear strength of reinforced concrete beams. *Journal of American Concrete Institute* **60(1)**: 51–72.

BSI (British Standards Institution) (1997) BS 8110. Part 1: Structural use of concrete: code of practice for design and construction. BSI, London.

BSI (2004) European Standard EN-1992-1-1:2004. Eurocode 2: Design of concrete structures. Part 1, general rules and rules for buildings. BSI, 2004, London.

Cheng G, Tan KH and Cheong HK (2001) Shear behaviour of large reinforced concrete deep beams. Paper 1546 *EASEC8, 8th East Asia–Pacific Conference on Structural Engineering and Construction, Singapore*.

Clark AP (1951) Diagonal tension in reinforced concrete beams. *Journal of the American Concrete Institute* **23(2)**: 145–156.

Collins MP and Mitchell D (1991) *Prestressed Concrete Structures*, 1st edn. Prentice-Hall, Englewood Cliffs, New Jersey.

CEB–FIP (Comité Euro-International de Beton–Federation International de la Precontrainte) (1993) *Model Code for Concrete Structures*. Thomas Telford, London.

de Cossio RD and Siess CP (1960) Behavior and strength in shear of beams and frames without web reinforcement. *ACI Journal* **56(2)**: 695–735.

DIANA (2005) *User's manual released notes* (Frits C de Witte and and Gerd-Jan Schreppes (eds)). TNO DIANA BV, Delft.

Kong YL and Rangan BV (1998) Shear strength of high-performance concrete beams. *ACI Structural Journal* **94(6)**: 677–688.

Kong FK, Robins PJ and Cole DF (1970) Web reinforcement effects on deep beams. *ACI Journal* **67(73)**: 1010–1017.

Lehwalter N (1988) *The Bearing Capacity of Concrete Compression Struts in Strut and Tie Models with Examples of Deep Beams*. PhD thesis, Technical University of Darmstadt, Germany.

Leonhardt F and Walter R (1964) The Stuttgart shear tests, 1961: contributions to the treatment of the problems of shear in reinforced concrete construction. Cement and Concrete Association.

Mathey RG and Watsein D (1963) Shear strength of beams without web reinforcement containing deformed bars of different yield strengths. *ACI Journal* **60(2)**: 183–207.

Moody KG, Viest IM, Ester RC and Hognestad E (1954) Shear

strength of reinforcement concrete beams. Part 1: test simple beams. *ACI Journal* **26(4)**: 317–332.

Oh JK and Shin SW (2001) Shear strength of reinforced high-strength concrete deep beams. *ACI Structural Journal* **98(2)**: 164–173.

Placas A (1969) *Shear Strength of Reinforced Concrete Beams*. PhD thesis, Imperial College of Science and Technology, London.

Rawdon de Paiva HA and Siess CP (1965) Strength and behavior of deep beams in shear. *Journal of the Structural Division, ASCE* **91(ST5)**:19–41.

Regan PE (1971) Shear in reinforced concrete – an experimental study. Report to the Construction Industry and Information Association (CIRIA).

Reyes de Ortiz I (1993) *Strut and Tie Modelling of Reinforced Concrete Short Beams and Beam-Column Joints*. PhD thesis, University of Westminster, London.

Sagaseta J (2008) *The Influence of Aggregate Fracture on the Shear Strength of Reinforced Concrete Beams*. PhD Thesis, Imperial College London, London.

Sarsam KF and Al-Musawi JM (1992) Shear design of high-and normal strength concrete beams with web reinforcement. *ACI Structural Journal* **89(6)**: 658–664.

Schlaich J, Jennewein M and Schafer K (1987) Towards a consistent design of structural concrete. *PCI Journal* **32(3)**: 74–150.

Smith KN and Vantsiotis AS (1982) Shear strength of deep beams. *ACI Journal* **79(22)**: 201–213.

Tan KH, Kong FK, Teng S and Guan S (1995) High-strength concrete deep beams with effective span and shear span variations. *ACI Structural Journal* **92(4)**: 395–405.

Tan KH, Kong FK, Teng S and Weng LW (1997) Effect of web reinforcement of high-strength concrete deep beams. *ACI Structural Journal* **94(5)**: 572–582.

Tan KH and Lu HY (1999) Shear behavior of large reinforced concrete deep beams and code comparisons. *ACI Structural Journal* **96(5)**: 836–845.

Vollum RL and Tay UL (2001) Strut and tie modelling of shear failure in short-span beams. *Concrete Communication Conference*, UMIST, Manchester, British Cement Association/Concrete Society, pp. 193–199.

Walraven JC and Lehwalter N (1994) Size effects in short beams loaded in shear. *ACI Structural Journal* **91(5)**: 585–593.

Zhang N and Tan KH (2007) Size effect in RC deep beams: experimental investigation and STM verification. *Engineering Structures* **29(12)**: 3241–3254.

Discussion contributions on this paper should reach the editor by 1 October 2010